Effects of D X center and spatial distribution of electrons on the density of two-dimensional electron gas in modulation-doped AlGaAs/GaAs heterojunction structure

D. H. Lee and S. S. Li

Citation: Journal of Applied Physics **60**, 3789 (1986); doi: 10.1063/1.337546
View online: http://dx.doi.org/10.1063/1.337546
View Table of Contents: http://scitation.aip.org/content/aip/journal/jap/60/10?ver=pdfcov
Published by the AIP Publishing

Effects of *DX* center and spatial distribution of electrons on the density of two-dimensional electron gas in modulation-doped AlGaAs/GaAs heterojunction structure

D. H. Lee and S. S. Li
Department of Electrical Engineering, University of Florida, Gainesville, Florida 32611

(Received 6 June 1986; accepted for publication 29 July 1986)

The equilibrium density of two-dimensional electron gas in a modulation-doped AlGaAs/GaAs heterojunction structure has been studied by considering the deep electron traps (i.e., *DX* center) in doped AlGaAs layer, the spatial distribution of electrons in three conduction-band minima (Γ, L, and X), and the heavy doping effect. It is shown that the amount of conduction band-bending increases and the equilibrium density of two-dimensional electron gas decreases significantly as a result of incorporating these effects.

It is known that the two-dimensional electron gas (TEG) at an abrupt interface between the highly n-doped AlGaAs and the undoped GaAs exhibits very high electron mobilities (e.g., for AlGaAs/GaAs, 2.4×10^6 cm^2/V s at 4.2 K and 2.05×10^5 cm^2/V s at 77 K),[1] resulting from the reduced ionized impurity scattering in the channel by separating the electrons from their parent donor ions with a heterointerface.[2] In application of this TEG to the high-speed electronic or photonic devices, it is of paramount importance to optimize the density of TEG, which is strongly dependent on the doping concentration in doped AlGaAs layer, the aluminum mole fraction of $Al_xGa_{1-x}As$, the deep/shallow electron traps, charge states at the heterointerface, and the thickness of undoped AlGaAs layer.

For the calculation of the equilibrium density of TEG, several models have been made by the assumption of depletion approximation,[3] employing the degeneracy of free carriers,[4] and considering the coexistence of shallow and deep donors.[5] However, the effects of deep electron traps and aluminum mole fraction to the density of TEG, which are quite significant, have been neglected or oversimplified in their works. The deep electron trap (the so-called *DX* center) is known to be inevitably incorporated with a very high concentration comparable to that of the dopant impurity.[6,7] As a result, this kind of electron trap produces additional space charges in the depletion region, a variation of threshold voltage with a temperature, and an instability of current-voltage characteristics to illumination.[8] In practice, the aluminum mole fraction, as an adjustable parameter, is in the range of 20–45% to maximize the concentration of free electrons and to suppress any appreciable reinjection of confined TEG. Therefore, one must take into account the following variations as a function of aluminum mole fraction: (1) spatial distribution of electrons in both direct and indirect conduction-band minima (Γ, L, and X),[9] (2) density of deep electron traps, and (3) band-gap discontinuity.

The purpose of this communication is to calculate more accurately the conduction-band bending of AlGaAs and the equilibrium density of TEG by considering the effects of positively singly charged deep electron traps and spatial distribution of electrons. For the actual device applications, the AlGaAs layer is quite heavily doped. Thus, the heavy doping effects, such as carrier degeneracy and the decrease of activation energy of shallow dopant impurity, should also be considered.

Since the total charges depleted from the AlGaAs layer must be equal to the density of TEG at the heterointerface, one can start from the Poisson's equation in the space charge region of AlGaAs layer (see Fig. 1), which can be written as

$$\frac{d^2V(z)}{dz^2}=\frac{-\rho(z)}{\epsilon_0\epsilon_{r2}}$$

$$=(q/\epsilon_0\epsilon_{r2})\left[N_d^+(z)+N_t^+(z)-n(z)\right], \qquad (1)$$

where ϵ_{r2} is the dielectric constant of AlGaAs; $N_d^+(z)$, $N_t^+(z)$, and $n(z)$ are the concentrations of ionized donor impurities, unoccupied deep electron traps, and undepleted free electrons, respectively. In solving Eq. (1), each quantity of right-hand side is treated by considering the important factors cited above.

The undepleted free electrons can be represented by

$$n(z)=2N_c(\pi)^{-1/2}F_{1/2}\left[(E_f-E_c)/kT\right], \qquad (2)$$

where $F_{1/2}$ is a Fermi–Dirac integral of order 1/2; N_c is an

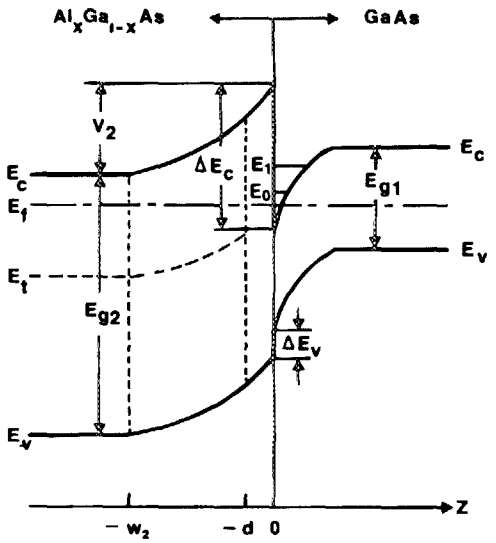

FIG. 1. One-dimensional schematic representation of AlGaAs/GaAs n$^+$-p abrupt heterojunction in thermal equilibrium (drawing is not in exact scale). d: undoped layer thickness; w_2: space-charge region boundary in AlGaAs region; V_2: total conduction-band bending; E_0, E_1: quantized electron energy levels.

 0021-8979/86/223789-03$02.40

effective density of states in the conduction band. Here, if we consider the spatial distribution of electrons in both direct and indirect conduction-band minima with a parabolic density of states, then

$$N_c = 2(2\pi kT/h^2)^{3/2}\{(m_n^\Gamma)^{3/2} + (m_n^L)^{3/2}\exp[(-E^{L-\Gamma})/kT] + (m_n^X)^{3/2}\exp[(-E^{X-\Gamma})/kT]\}, \quad (3)$$

where m_n^Γ, m_n^L, and m_n^X are the density of effective masses for the three conduction-band minima Γ, L, and X, respectively; $E^{L-\Gamma} = E_g^L - E_g^\Gamma$ and $E^{X-\Gamma} = E_g^X - E_g^\Gamma$.

The unoccupied deep electron traps, which have a strong compensation effect, can be written as

$$N_t^+ = N_t(1 - 1/\{1 + g_t \exp[(E_t - E_f)/kT]\}), \quad (4)$$

where g_t is a degeneracy factor; N_t and E_t are the density and activation energy of deep electron traps (e.g., for the SI DX center, $E_t \simeq 0.43$ eV), respectively.

The ionized shallow impurity concentration may be expressed by

$$N_d^+ = N_d(1 - 1/\{1 + g_d \exp[(E_d - E_f)/kT]\}), \quad (5)$$

where g_d and N_d denote the degeneracy factor and density of dopant impurity, respectively; E_d is the donor activation energy, which is a function of alloy composition ratio, and diminishes as N_d approaches to N_c.

After solving the Poisson's equation, one can construct the conduction band structure and electric field distribution over the space-charge region. Thus, the contributions of electron traps and the spatial distribution of electrons to the total conduction-band bending can be estimated as functions of doping concentration and density of deep electron traps. As is shown in Fig. 2, the band bending becomes more significant as the density of deep electron traps increases. Furthermore, the temperature-dependent threshold voltage of modulation-doped field-effect transistors (MODFETs)[10] can also be predicted.

Next, for the conduction-band notch on the GaAs side, the TEG can be related to the Fermi level by employing the triangular well and quasi-constant electric field. Thus, the solution for the longitudinally quantized energy level can be approximated by[11]

$$E_n(\text{eV}) = (h^2/2m_l^*)^{1/3}(3\pi q\mathscr{E}_i/2)^{2/3}(n + 3/4)^{2/3}, \quad (6)$$

where m_l^* is the longitudinal effective mass; $\mathscr{E}_i$ is the electric field at the interface. If we consider only two lowest subbands for the triangular well, the density of TEG can be related to the Fermi level by

$$\begin{aligned} n_s &= D\int_{E_0}^{E_1} dE\Big/\{1 + \exp[(E - E_f/kT]\} \\ &\quad + 2D\int_{E_1}^{\infty} dE\Big/\{1 + \exp[(E - E_f)/kT]\} \\ &= DkT\log(\{1 + \exp[(E_f - E_0)/kT]\} \\ &\quad \times\{1 + \exp[(E_f - E_1)/kT]\}), \end{aligned} \quad (7)$$

where $D = qm^*/\pi h^2$ is the density of states for a two-dimensional system with a single quantized energy level.

From the Gauss law at the heterointerface, the density of TEG becomes

$$n_s = (\epsilon_0\epsilon_{r2}/q)\mathscr{E}_2(0). \quad (8)$$

If we consider any charge state Q_i at the heterointerface, Eq. (8) must be modified as

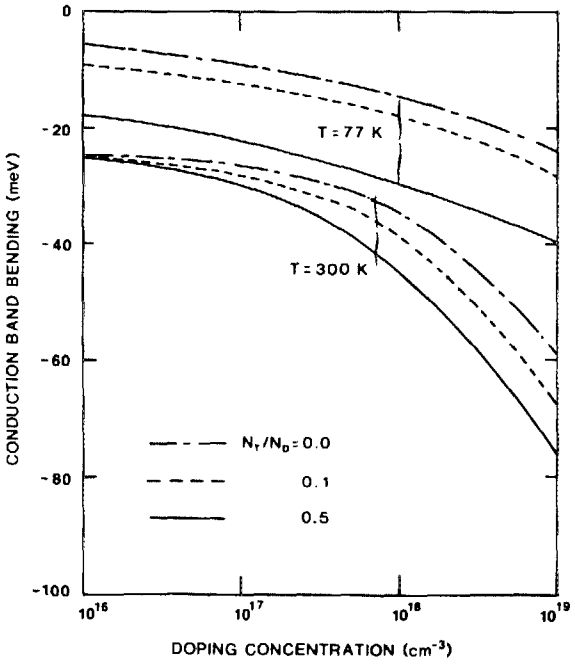

FIG. 2. Conduction-band bending due to the deep electron traps, the spatial distribution of electrons ($x = 0.3$) and the heavy doping effects, as functions of doping concentration and density of deep electron traps ($E_t = 0.43$ eV) at 77 and 300 K. Undoped layer thickness = 0.

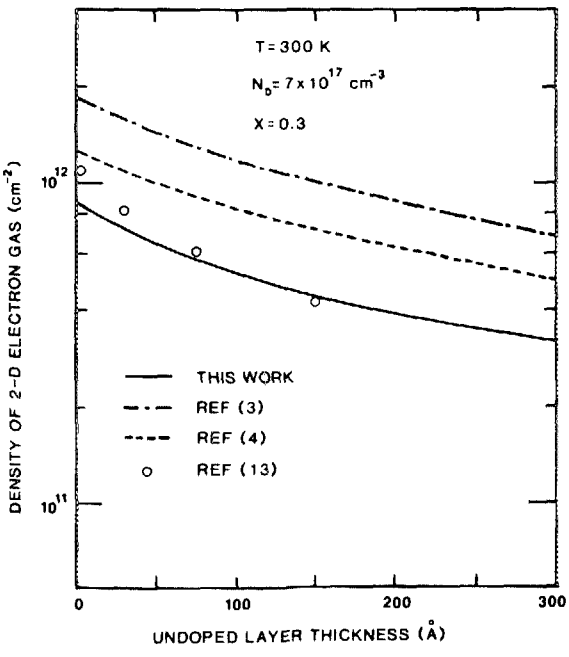

FIG. 3. Density of two-dimensional electron gas as a function of undoped layer thickness compared with the theoretical works of Delagebeaudeuf and Linh (Ref. 3), Lee *et al.* (Ref. 4), and the experimental data of Delagebeaudeuf *et al.* (Ref. 13) for $N_t/N_d = 0.1$.

$$n_s = (\epsilon_0 \epsilon_{r2}/q)\mathscr{E}_2(0) - Q_i/q, \quad (9)$$

where $\mathscr{E}_2(0)$ is the electric field at the heterointerface and is obtained from Eq. (1).

To calculate the density of TEG, one must solve Eqs. (7) and (8) [or (9)] simultaneously with the boundary condition

$$V(+0) = V(-0) + \Delta E_c/q, \quad (10)$$

where ΔE_c is the conduction-band discontinuity, which is assumed equal to $0.6\Delta E_g$.[12] Figure 3 shows the calculated equilibrium density of TEG as a function of undoped layer thickness of a modulation-doped AlGaAs/GaAs heterojunction structure along with the published calculations and experimental data. Our theoretical calculations show a considerable reduction of the density of TEG as a result of incorporating the effects cited in this communication, which yield an excellent agreement with the published experimental data, as cited in Ref 13.

In conclusion, our results show that the deep electron traps, the spatial distribution of electrons as a function of aluminum mole fraction, and the heavy doping effect are important parameters which should be included in the calculation of the equilibrium density of TEG.

This work was supported by the Air Force Office of Scientific Research under Grant No. AFOSR-81-0187.

[1]S. Hiyamizu, J. Saito, K. Kondo, T. Yamamoto, T. Ishikawa, and S. Sasa, J. Vac. Sci. Technol. B **3**, 585 (1985).
[2]L. Esaki and R. Tsu, IBM Research Internal Report RC 2418 (1969).
[3]D. Delagebeaudeuf and N. Linh, IEEE Trans. Electron Devices **ED-29**, 955 (1982).
[4]K. Lee, M. Shur, T. Drummond, and H. Morkoç, J. Appl. Phys. **54**, 2093 (1983).
[5]S. Subramanian, A. S. Vengurlekar, and A. Diwan, IEEE Trans. Electron Devices **ED-33**, 707 (1986).
[6]D. V. Lang, R. A. Logan, and M. Jaro, Phys. Rev. B **19**, 1015 (1979).
[7]A. Valois and G. Robinson, J. Vac. Sci. Technol. B **3**, 649 (1985).
[8]H. Morkoc and P. Solomon, IEEE Spectrum **2**, 28 (1984).
[9]S. Adachi, J. Appl. Phys. **58**, R1 (1985).
[10]T. J. Drummond, H. Morkoc, K. Lee, and M. S. Shur, IEEE Trans. Electron. Device Lett. **EDL-3**, 338 (1982).
[11]L. Laudau and E. Lifshitz, *Quantum Mechanics* (Oxford University, New York, 1977).
[12]R. C. Miller, A. C. Gossard, D. A. Kleiman, and O. Munteanu, Phys. Rev. B **29**, 3740 (1984).
[13]D. Delagebeaudeuf, P. Delescluse, P. Etienne, M. Laviron, J. Chaplart, and N. Linh, Electron. Lett. **16**, 667 (1980).

Performance characteristics of the ArF excimer laser using a low-pressure argon-rich mixture

Akira Suda, Minoru Obara, and Akira Noguchi
Department of Electrical Engineering, Faculty of Science and Technology, Keio University, 3-14-1 Hiyoshi, Kohoku-ku, Yokohama 223, Japan

(Received 12 May 1986; accepted for publication 7 August 1986)

Low-pressure operation of an electron-beam excited ArF laser was experimentally compared to KrF lasers, both of which were pumped at high excitation rate by a 65 ns electron beam. We obtained the ArF laser energy of 95 J with an intrinsic efficiency of 3.4% from a 650 Torr Ar/F_2 mixture pumped at an excitation rate of 2.3 MW/cm^3. In the low-pressure region (near one atmosphere) the Ar/F_2 mixture gave higher efficiency than that of Ne-buffered mixtures, and moreover gave higher efficiency than those of the KrF lasers operating with various mixtures under the same excitation rate. As a result, the ArF laser operating in this regime is found to be a better candidate than the KrF laser as an inertial confinement fusion driver.

Rare-gas halide lasers, particularly KrF lasers (248 nm) have intensively been developed as an inertial confinement fusion (ICF) energy driver.[1-3] Atmospheric-pressure operation of the KrF laser is preferred because it can reduce many technical difficulties when the scaled up versions of these amplifiers are built. We previously proposed that the electron-beam (*e*-beam) excited KrF laser with atmospheric-pressure Kr-rich mixtures can operate efficiently with high specific output energy.[4-8] The shorter wavelength ArF laser (193 nm) has a potential of producing high power output and comes to be attractive for use as an ICF driver because the shorter wavelength beams can be more efficiently absorbed by a fuel pellet.[9]

The ArF laser was first demonstrated by Hoffman *et al.*[10] They obtained a laser energy of 92 J from a 1400 Torr mixture of Ar/F_2 pumped by a 50 ns *e*-beam with an intrinsic efficiency of 3%. Murray and Powell used Ne as the buffer gas and obtained an intrinsic efficiency of 5% by a 50 ns *e*-beam pumping.[11] Since then, most of works on the *e*-beam excited ArF laser have been performed preferably using high-pressure Ne-buffered mixtures and higher efficiency was achieved with Ne-buffered mixtures than Ar/F_2 mixtures.[12-14] That may be due to the fact that the ArF^* is less quenched by Ne than Ar.[15] However, the ArF^* formation efficiency in the Ar/F_2 system is essentially as high as the KrF^* formation efficiency. Our previous work showed that

 0021-8979/86/223791-03$02.40